Chemical Engineering Journal 161 (2010) 106–113

Contents lists available at ScienceDirect

Chemical Engineering Journal

journal homepage: www.elsevier.com/locate/cej

As(V) and As(III) removal from water by a Ce–Ti oxide adsorbent: Behavior and mechanism

Zhijian Li[a,b], Shubo Deng[a,b,*], Gang Yu[a,b], Jun Huang[a,b], Veronica Chao Lim[a,b]

[a] Department of Environmental Science and Engineering, Tsinghua University, Beijing 100084, China
[b] Persistent Organic Pollutants (POPs) Research Center, Tsinghua University, Beijing 100084, China

ARTICLE INFO

Article history:
Received 25 February 2010
Received in revised form 20 April 2010
Accepted 20 April 2010

Keywords:
Ce–Ti oxide adsorbent
Sorption capacity
Sorption mechanism
As(V)
As(III)

ABSTRACT

Since As(V) and As(III) usually occur in groundwater simultaneously, the synthesis of novel adsorbents for both As(V) and As(III) removal is attractive. In this paper, a Ce–Ti hybrid oxide adsorbent with high sorption capacities for As(V) and As(III) was successfully prepared using a two-step reaction. Environmental scanning electron microscopy (ESEM) revealed that the Ce–Ti oxide adsorbent was composed of nanoparticles in the size range of 100–200 nm. Sorption isotherms show that the powdered adsorbent had high sorption capacity up to 7.5 mg/g for As(V) and 6.8 mg/g for As(III) at the equilibrium arsenic concentration of 10 μg/L, higher than most reported adsorbents. The optimum adsorption capacity on the adsorbent was achieved at pH below 7 for As(V) and at neutral pH for As(III). Fourier transform infrared (FTIR) analysis indicated that the hydroxyl groups on the adsorbent surface were involved in arsenic adsorption, while X-ray photoelectron spectroscopy (XPS) provided further evidence for the involvement of hydroxyl groups in the sorption and the formation of monodentate and bidentate complexes on the adsorbent surface.

1. Introduction

High arsenic concentration in groundwater has become a major concern for many years in countries such as Bangladesh, India, and China. Adsorption is regarded as one of the most promising techniques for arsenic removal from water, and many adsorbents such as activated alumina, iron (hydr)oxide, Mg–Fe, Mn–Al, and Fe–Ce bimetal oxides have been reported to be effective for arsenic removal [1–5]. Activated alumina is often used for arsenic removal, but has disadvantages including aluminum dissolution, relatively low sorption capacity and low optimum pH, which prevent it from wide application [1]. In recent years, iron-based adsorbents have been developed and used to remove arsenic from water [2–4]. In general, both As(V) and As(III) occur in groundwater, but some reported adsorbents are not effective for their simultaneous removal, having low sorption capacity for As(III) [6–8]. Therefore, developing effective adsorbents for both As(V) and As(III) removal from drinking water is desirable from the viewpoint of actual pollution.

Sorption capacity is one of the important characteristics in the evaluation of adsorbents used in arsenic removal from water. To increase the sorption capacity of arsenic, some novel adsorbents have been prepared including nanocrystalline TiO_2 adsorbent prepared by the hydrolysis of titanium salts, which had a higher sorption capacity for As(V) and As(III) than other conventional adsorbents [9]. Cumbal and Sengupta reported an iron oxide loaded resin with a high sorption capacity for As(III) and As(V) [10]. Arsenic removal using a polymeric ligand exchanger prepared by loading Cu^{2+} to commercially available resin also was reported to have good sorption for As(V) [11]. Previous studies have showed that the incorporation of La(III), Ce(III) and Mn(IV) into the iron oxide and waste gels could significantly increase the sorption capacity for arsenic [12,13]. Although considerable work has been done on the preparation of aluminum or iron-based bimetal adsorbents, less is known about TiO_2-based adsorbents for arsenic removal. The incorporation of other metals or organic materials into the lattice structure of TiO_2 might increase arsenic sorption capacity.

Most previous studies have suggested that the sorption mechanism of arsenic on adsorbents occurs through anion exchange, but experiments and analysis did not provide clear evidence for this conclusion. Recent analytical techniques such as FTIR, XPS, and extended X-ray absorption fine structure spectroscopic (EXAFS) analysis are capable of providing better and quantitative information into the sorption mechanism of arsenic [6,7,12]. Goh et al. reported that Mg/Al layered double hydroxide exhibited enhanced As(V) removal through anion exchange with possible formation of outer-sphere complexes and ligand exchange with formation of inner-sphere complexes [7]. Pena et al. suggested the efficient

* Corresponding author at: Department of Environmental Science and Engineering, Tsinghua University, No. 1 Qinghua Yuan, Haidian District, Beijing 100084, China. Tel.: +86 10 62792165; fax: +86 10 62794006.
E-mail address: dengshubo@tsinghua.edu.cn (S. Deng).

1385-8947/$ – see front matter © 2010 Elsevier B.V. All rights reserved.
doi:10.1016/j.cej.2010.04.039

removal of As(V) and As(III) by nanocrystalline TiO_2 due to its high surface area and the presence of high affinity surface hydroxyl groups through FTIR and EXAFS analysis [14]. However, the sorption mechanism of arsenic on the modified-TiO_2 adsorbent has not been reported in the literature.

In this study, a novel Ce–Ti hybrid oxide adsorbent with high sorption capacity for both As(V) and As(III) was prepared and used to remove arsenic from water. Sorption behavior, especially sorption capacity, was investigated in detail. The adsorbents before and after arsenic sorption were characterized by ESEM, FTIR and XPS, and the possible sorption mechanisms were discussed.

2. Materials and methods

2.1. Materials

Chemicals including $Ti(SO_4)_2$, polyvinyl alcohol (PVA), and $Ce(NO_3)_3{\cdot}6H_2O$ were purchased from Sigma–Aldrich Co. 1000 mg/L of arsenic stock solution was prepared by dissolving $Na_2HAsO_4{\cdot}7H_2O$ or $NaAsO_2$ in deionized water.

2.2. Preparation of the Ce–Ti hybrid adsorbent

A typical synthesis process via hydrolysis and subsequent precipitation was performed as follows: hydrous TiO_2 ($TiO_2{\cdot}xH_2O$) precipitate was first produced by the hydrolysis of 0.2 M $Ti(SO_4)_2$ solution in the presence of 0.16% PVA at 80 °C in a thermostatic water bath for 2 h, and then $Ce(NO_3)_3$ solution was added to reach 0.02 M, followed by a pH adjustment to about 8 through the addition of NaOH solution. The resulting precipitates were filtered and washed with deionized water and finally heated in an oven at 80 °C until the sample reached constant weight. The dried adsorbent was crushed and screened, and the adsorbent particles smaller than 0.074 mm in diameter were used as powder adsorbent, while the adsorbent in the size range of 0.28–0.60 mm was defined as granular adsorbent. For the control study, pure hydrous TiO_2 was prepared by the hydrolysis method, while pure hydrous cerium oxide was obtained by the precipitation method according to the same process described above.

2.3. Batch sorption experiments

Batch sorption experiments were conducted to examine the sorption kinetics, sorption isotherm, as well as the effect of solution pH on arsenic sorption. All sorption experiments were carried out in 250 mL flasks, each containing 100 mL As(V) or As(III) solution by the addition of arsenic stock solution in deionized water. After the addition of 0.01 g of adsorbent each, the flasks were shaken under dark condition in a thermostatic shaker at 150 rpm and 25 °C for 12 h (a kinetic study showing that the sorption equilibrium of As(V) and As(III) was achieved within 12 h). In the investigation of sorption isotherms, the initial arsenic concentrations ranged from 20 μg/L to 20 mg/L, and pH values were adjusted to 6.5 and kept constant throughout the sorption experiment by adding HCl and NaOH solutions at regular time intervals. The effect of pH on arsenic sorption was conducted in 5 mg/L As(V) or As(III) solution at an initial pH ranging from 4 to 10, and the final solution pH was measured.

After adsorption, the adsorbent was separated from the solution by filtration through a 0.22 μm membrane, and the residual arsenic concentration in the filtrate was measured with an inductively coupled plasma optical emission spectrometry (ICP-OES, IRIS Interpid II XSP, USA). If the measured arsenic concentration was below 1 mg/L, graphite furnace atomic absorption spectroscopy was utilized.

2.4. Adsorbent regeneration and reuse

0.01 g adsorbent was added into 100 mL of 5 mg/L As(V) or As(III) solution at pH 6.5, and the flask was shaken at 150 rpm in a thermostatic shaker at 25 °C for 12 h. After adsorption, the As-loaded adsorbent was filtered and rinsed with water. In the desorption test, the spent adsorbent was put into 100 mL of 0.5 M NaOH solution in a 250-mL flask, and the mixture was shaken at 150 rpm at 25 °C for 12 h. After the desorption process, the adsorbent was filtered, and the arsenic concentration in filtrate was analyzed. The regenerated adsorbent was washed with deionized water until neutral pH was reached, and then the adsorbent was filtered and dried at 50 °C for reuse in the next cycle. The adsorption–desorption cycles were repeated five times, and the sorption capacity for arsenic in each sorption experiment was calculated.

2.5. Morphology observation

The surface morphology of the granular Ce–Ti adsorbent was observed using an environmental scanning electron microscope (FEI Quanta 200 FEG, Netherlands).

2.6. Zeta potential measurement

A 0.1 g portion of the adsorbent before and after arsenic sorption was placed into 100 mL of deionized water and stirred for 12 h. The solution pH was adjusted with 0.1 M NaOH or HCl solution to a desired value. After 1 h of stabilization, the final solution pH was recorded, and the supernatant was then decanted and used to conduct zeta potential measurements with a Delsa NanoC Zeta potential instrument (Beckman Coulter, USA). All data were determined five times, and the average value was adopted.

2.7. FTIR spectroscopy

The samples of the Ce–Ti adsorbent before and after As(V) and As(III) sorption were blended with KBr, and then pressed into disks for FTIR analysis. The spectra were recorded on a FTIR spectrophotometer (Nicolet 6700, USA) in the wavenumber range of 400–4000 cm^{-1} under ambient conditions.

2.8. XPS analysis

The Ce–Ti adsorbent before and after As(V) and As(III) sorption were analyzed using XPS (PHI Quantera 5300X, Japan) with an Al Kα X-ray source (1486.71 eV of photons) to determine the C, O, Ce, Ti and As contents on the adsorbent surface. The X-ray source was run at a reduced power of 150 W, and the pressure in the analysis chamber was maintained at less than 10^{-8} Torr during each measurement. All binding energies were referenced to the neutral C1s peak at 284.8 eV to compensate for surface charge effects. The software package XPSpeak 4.1 was used to fit the XPS spectra peaks, and the full width at half-maximum was maintained constant for all components in a given spectrum.

3. Results and discussion

3.1. Adsorbent characterization

In the adsorbent preparation experiments, different modified-TiO_2 adsorbents were prepared in the presence of $AlCl_3$, $Ce(NO_3)_3$, $FeCl_3$, $Zr(SO_4)_2$, or $La(NO_3)_3$, through precipitation or hydrolysis methods. It was found that the novel Ce–Ti adsorbent obtained by hydrolysis and subsequent precipitation had the highest sorption capacity for both As(V) and As(III) among the modified adsorbents. The preparation of Ce–Ti adsorbent was optimized for Ti/Ce ratio,

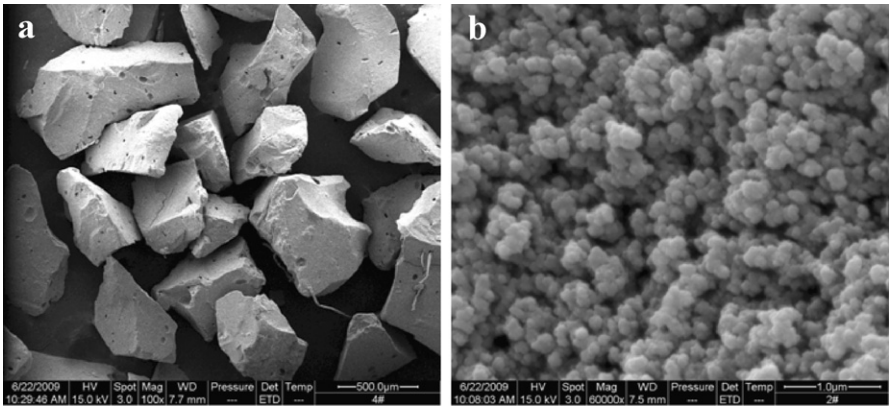

Fig. 1. ESEM micrographs of the granular pristine Ce–Ti oxide adsorbent at (a) low and (b) high magnification.

PVA concentration, and drying temperature in our previous study [15]. The adsorbent used in this study was prepared under the optimized conditions shown in Section 2. Due to the presence of PVA, the granular adsorbent had a strong mechanical strength and could be directly used in the column study.

The granular Ce–Ti adsorbent was observed by ESEM, and the micrographs are shown in Fig. 1. As presented in Fig. 1a, the granular adsorbent had an irregular shape, but the adsorbent surface was smooth. Fig. 1b shows an enlarged image on the surface of the granular adsorbent, and the nanoparticles in the size range of 100–200 nm as well as some aggregates were observed. If no PVA was added in the solution during the adsorbent preparation, the adsorbent was composed of large particles above 1 μm diameter [15]. Evidently, PVA not only increased the mechanical strength of the granular adsorbent, but also facilitated the formation of nanoparticles during the hydrolysis process. The specific surface area of the Ce–Ti adsorbent was measured to be 137.4 m^2/g using the Brunauer–Emmett–Teller method. The total pore volume was 0.267 cm^3/g, and the micropore and mesopore surface areas were 60.8 m^2/g and 38.2 m^2/g respectively, indicating a porous structure in the Ce–Ti adsorbent. The ESEM-EDX analysis showed that the Ti/Ce molar ratio on the adsorbent surface was about 8.6, which was close to the reactant content in the preparation. The surface charge and functional groups on the adsorbent were also analyzed using zeta potential, FTIR and XPS spectra in the following sections.

In addition, X-ray diffraction analysis showed that no strong peaks were found in the spectrum, indicating an amorphous phase in the hybrid adsorbent. It should be noted that the weak crystalline phase of the Ce–Ti hybrid adsorbent may be attributed to the interference of PVA in the preparation and low drying temperature. The high sorption capacity of arsenic on the Ce–Ti adsorbent may be related to its amorphous structure and the hydroxyl groups on the adsorbent surface. Wu et al. also reported that the amorphous Fe–Al–Ce adsorbent also had a high sorption capacity for fluoride, but the sorption capacity decreased significantly when this adsorbent formed a crystalline structure at high calcination temperatures [16]. It has been reported that the adsorption capacity of As(III) onto the calcined sanding waste decreased at high calcination temperatures due to the decreased surface area and highly developed crystallinity [17].

3.2. Effect of solution pH

Fig. 2a shows the effect of equilibrium pH on As(V) and As(III) sorption onto the powder Ce–Ti adsorbent, and their sorption profiles are completely different. The adsorbed amount of As(III) on the adsorbent first increased and then decreased with increasing solution pH, and the highest sorption capacity of 35.1 mg/g was achieved at pH 7.1. The adsorbent had a relatively high sorption capacity for As(III) in the whole pH range studied. By contrast, the adsorption capacity of As(V) was high and stable at pH values from 4.1 to 6.8, but decreased rapidly from 39.7 mg/g to 3.5 mg/g when the solution pH increased from 6.8 to 9.8. It has been reported that other adsorbents such as TiO_2 and Ce–Fe adsorbents also have low sorption capacities for As(V) under alkaline conditions [18,19].

The different sorption capacities of As(V) and As(III) on the adsorbent are related to the adsorbent surface charge and arsenic species in solution at different pH values. It is well known that As(V) mainly exists as its anionic forms within the pH range from 4 to 10 ($H_2AsO_4^-$ as the main species at pH from 3 to 6, $HAsO_4^{2-}$ and AsO_4^{3-} as major species at pH above 8), while As(III) is present

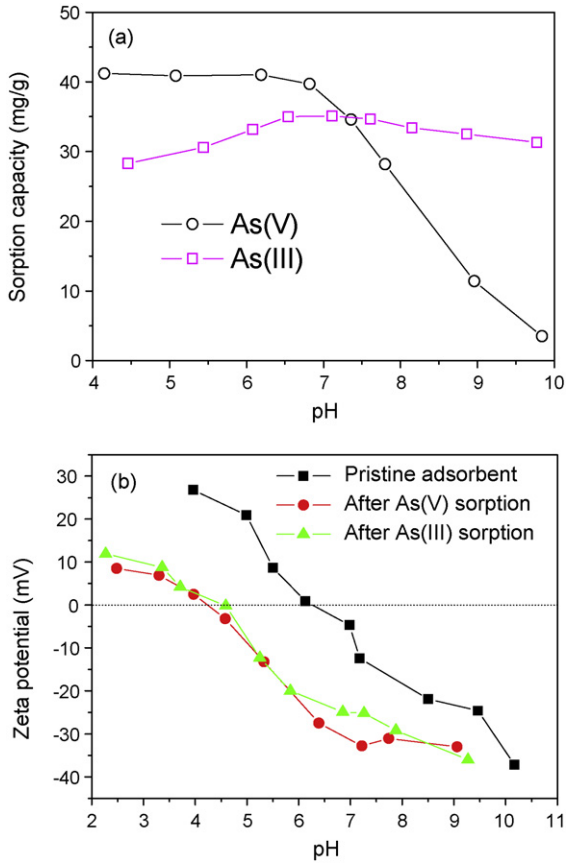

Fig. 2. Effect of pH on (a) arsenic sorption on the Ce–Ti oxide adsorbent and (b) zeta potential before and after arsenic sorption.

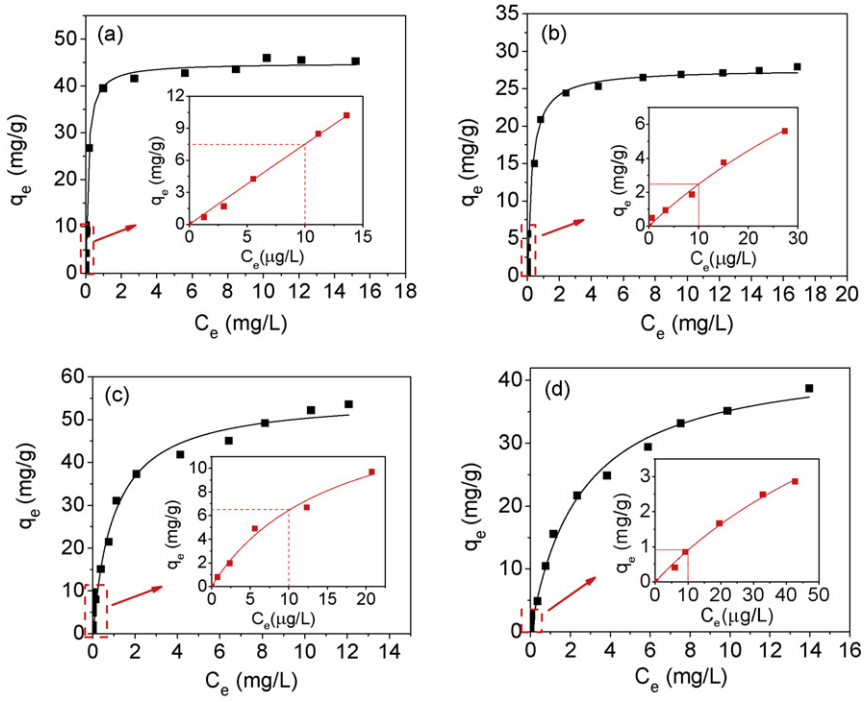

Fig. 3. Sorption isotherms of As(V) and As(III) on the powder and granular Ce–Ti oxide adsorbent at pH 6.5. (a) As(V) sorption on powder adsorbent, (b) As(V) sorption on granular adsorbent, (c) As(III) sorption on powder adsorbent and (d) As(III) sorption on granular adsorbent.

as neutral $HAsO_2$ at pH below 8 and $H_2AsO_3^-$ becomes dominant at pH above 9.2 [10]. Solution pH also affects the adsorbent surface charge. The zeta potentials of the adsorbent as a function of solution pH are shown in Fig. 2b, and it can be seen that the Ce–Ti adsorbent has a zero point of zeta potential at pH 6.2, suggesting that the adsorbent surface is positive at pH below 6.2, and the adsorbent is favorable for anionic As(V) removal from water from the viewpoint of electrostatic attraction. However, the As(V) sorption on the adsorbent at pH above 6.2 cannot be interpreted via the electrostatic interaction since the electrostatic interaction between the adsorbent and As(V) should be electrically repulsive, and other interactions may be involved instead. Similarly, electrostatic attraction is impossible in As(III) sorption on the adsorbent. At low pH, some hydroxyl groups were protonated and were not involved in the sorption of As(III) on the adsorbent, leading to a lower sorption capacity for As(III), while the decrease in sorption capacity at high pH was attributed to the electrostatic repulsion between $H_2AsO_3^-$ and an anionic adsorbent surface. However, the adsorbent had high sorption capacity for As(III) over a wide pH range. One possible reason is that the hydroxyl groups on the adsorbent surface played a dominant role in the sorption process, which will be fully discussed in Section 3.5.

3.3. Sorption capacity

The Ce–Ti hybrid adsorbent used in this study had a sorption capacity of 41.3 mg/g for As(V) when 0.01 g adsorbent was added in 100 mL of 5 mg/L As(V) solution at pH 6 for 12 h. By contrast, a pure TiO_2 adsorbent was also prepared in the presence of PVA using the hydrolysis method, and its sorption capacity for As(V) was only 20.1 mg/g under the same sorption conditions; the pure cerium oxide adsorbent obtained by the precipitation method had a sorption capacity of 24.9 mg/g. Obviously, the Ce–Ti hybrid oxide adsorbent had a much higher sorption capacity than the pure TiO_2 and cerium oxide adsorbents, indicating the synergistic effect of Ti and Ce oxides in the sorption process.

Fig. 3 shows the sorption isotherms of As(V) and As(III) on the powder and granular Ce–Ti oxide adsorbents. It can be seen that the adsorbent had a high sorption capacity for both As(V) and As(III). To determine the maximum sorption capacity, the Langmuir model was used to fit the experimental data. As shown in Fig. 3a–d, this model successfully described the adsorption of As(V) and As(III) on the powder and granular adsorbents. The maximum sorption capacity on the powder adsorbent was 44.9 mg/g for As(V), and 55.3 mg/g for As(III). It is interesting that their sorption isotherms exhibited different profiles. The maximum sorption capacity of As(V) on the powder adsorbent was achieved at low equilibrium concentration, while the adsorbed amount of As(III) increased gradually, and the maximum sorption capacity was not obtained in the concentration range studied. In addition, the sorption capacity of As(V) and As(III) on the granular adsorbent was lower than that of the powder adsorbent.

The maximum sorption capacities of arsenic on the adsorbents were usually obtained at high arsenic concentration and used to evaluate the adsorbents [20]. However, the sorption capacity of arsenic at low equilibrium concentration is extremely important in actual drinking water treatment since arsenic concentration in raw groundwater is normally below 100 μg/L and the final arsenic concentration in drinking water must be below 10 μg/L. Fig. 3 demonstrates the sorption capacity of As(V) and As(III) on the powder and granular adsorbent at the equilibrium arsenic concentration of 10 μg/L. The sorption capacities of As(V) on the powder and granular adsorbent were 7.5 mg/g and 2.5 mg/g, respectively. The sorption capacity for As(III) was about 6.8 mg/g on the powder adsorbent and 0.9 mg/g on the granular adsorbent.

Table 1 lists the sorption capacities of As(V) and As(III) on the different adsorbents as reported in the literature. Since the sorption capacities of arsenic on the reported adsorbents were obtained at different solution pH and equilibrium concentrations, it is difficult to make direct comparisons. Activated alumina is the most commonly used adsorbent in actual application for arsenic removal, but its sorption capacity for arsenic is not satisfactory. Iron-based adsorbents, especially the Fe–Mn and Ce–Fe binary oxides, had

Table 1
Comparison of adsorption capacity of arsenic on various adsorbents.

Sorbates	Adsorbents	Equilibrium concentration (mg/L)	Solution pH	Sorption capacity (mg/g)[a]	Ref.
As(V)	Activated alumina	1	7.2	8.8	[1]
	Ferric hydroxide[b]	0.01	6.5	1.1	[3]
	Granular ferric hydroxide (GFH)[b]	0.01	7.0	8	[21]
	Fe–Mn binary oxide	1.9	5.0	63.8	[12]
	Fe-Ce adsorbent	0.07	5.0	4.5	[18]
	ZrO_2 sphere[b]	0.01	6.4	0.8	[22]
	Zr-loaded resin[b]	0.2	4.0	19.5	[23]
	Aminated Fibers[b]	0.01	7.0	1.7	[6]
	Red mud	1	3.2	0.35	[24]
	Nanocrystalline TiO_2	0.15	7.0	11.2	[9]
	Powder Ce–Ti sorbent	0.01	6.5	7.5	This study
	Granular Ce–Ti sorbent	0.01	6.5	2.5	This study
As(III)	Activated alumina[b]	0.1	7.6	0.08	[25]
	Fe–Mn binary oxide	0.75	5.0	73.5	[12]
	MnO_2-loaded resin[b]	3	7.0–8.5	26	[26]
	Zr-loaded resin[b]	0.14	9.0	29.2	[22]
	Modified bauxite[b]	0.13	–	0.37	[27]
	Red mud	3	9.5	0.33	[24]
	Nanocrystalline TiO_2	0.6	7.0	8.3	[9]
	Powder Ce–Ti sorbent	0.01	6.5	6.8	This study
	Granular Ce–Ti sorbent	0.01	6.5	0.9	This study

[a] Calculated by the isotherm model or evaluated from the sorption isotherms.
[b] Granular adsorbent.

higher sorption capacities for As(V) and As(III). As shown in Table 1, the sorption capacity of As(V) and As(III) on the Fe–Mn binary oxide reached 63.8 mg/g at equilibrium concentration of 1.9 mg/L and 73.5 mg/g at 0.75 mg/L at pH 5, respectively. The granular ferric hydroxide had a sorption capacity up to 8 mg/g at the equilibrium arsenate concentration of 10 μg/L. When active components (MnO_2 and Zr(IV)) were loaded onto the porous materials such as activated carbon and resin, their sorption capacities for arsenic were enhanced. Although some natural adsorbents such as red mud are inexpensive, their sorption capacities for arsenic are very low. As presented in Table 1, the nanocrystalline TiO_2 prepared by hydrolysis had a sorption capacity of 11.2 mg/g for As(V) at the equilibrium concentration of 0.15 mg/L and 8.3 mg/g for As(III) at 0.6 mg/L, both of which are much higher than that of the commercial TiO_2 product [9]. The Ce–Ti oxide adsorbent prepared in this study possessed a higher sorption capacity for arsenic than the pure TiO_2 adsorbents. It should be noted that this hybrid adsorbent had a moderate sorption capacity for arsenic at high arsenic concentrations, but its sorption capacity at low equilibrium concentrations was much higher than other adsorbents except for GFH.

3.4. Regeneration and reuse

Regeneration of the spent adsorbent plays an important role in reuse of the adsorbent. Experiments were carried out to investigate the regeneration and reuse of the adsorbent for arsenic removal in the successive sorption–desorption cycles. HCl, HNO_3, NaOH, Na_2CO_3, and NaCl solutions were used to regenerate the spent Ce–Ti hybrid adsorbent in this study, and the preliminary result indicated that the 0.5 M NaOH solution was the best eluent for arsenic desorption from the spent adsorbent in terms of desorption kinetics and regeneration efficiency. Although the adsorbed arsenic could be desorbed from the adsorbent using a strong acid solution, the sorption capacity of arsenic on the regenerated adsorbent decreased significantly, indicating that some of the active components were resolved by the acid solution. After the regeneration in NaOH solution, the regenerated adsorbent was used in the next cycle, and the sorption capacities of the adsorbent for As(III) and As(V) in the successive five cycles are shown in Fig. 4. It was found that the sorption capacity of As(V) decreased from 40.9 mg/g to 36.6 mg/g after the first regeneration, and then remained relatively stable in the following four cycles. The sorption capacity of As(V) on the regenerated adsorbent was 33.2 mg/g in the fifth cycle. Similar regeneration efficiency was obtained for the As(III)-sorbed adsorbent, and the regenerated adsorbent had a sorption capacity of 25.3 mg/g for As(III) in the fifth cycle. No titanium and cerium ions were detected in the sorption and desorption process. The decrease in sorption capacity with cycle number may be due to the unsuccessful regeneration sites on the adsorbent. Clearly, the spent adsorbent was successfully regenerated in NaOH solution, and the Ce–Ti adsorbent had a good sorption capacity for arsenic in the subsequent cycles. The desorption of arsenic from the spent adsorbent may be due to the electrostatic repulsion between the adsorbent and anionic arsenic in NaOH solution.

3.5. Sorption mechanism

FTIR and XPS have been successfully used in previous studies to study surface interactions between adsorbates and adsorbents in the adsorption process [6,7,28,29]. The interactions between arsenic and the functional groups on adsorbents can be detected through the characteristic peak shift and intensity change in the FTIR and XPS spectra.

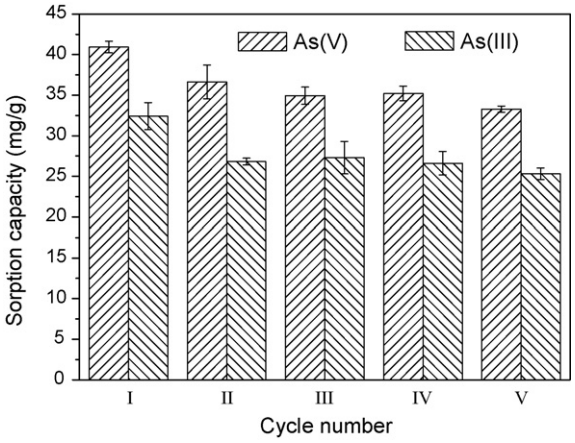

Fig. 4. Sorption capacity of As(V) and As(III) on the Ce–Ti oxide adsorbent in five successive adsorption–desorption cycles.

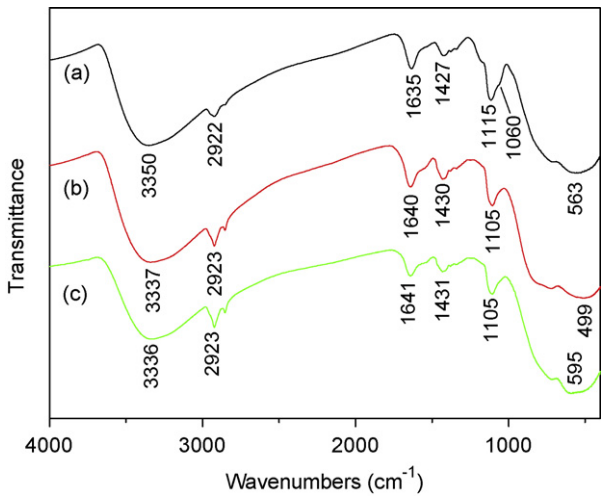

Fig. 5. FTIR spectra of the (a) Ce–Ti adsorbent, (b) As(V)-loaded Ce–Ti adsorbent, and (c) As(III)-loaded Ce–Ti adsorbent.

Fig. 5 presents the FTIR spectra of the Ce–Ti oxide adsorbent before and after As(V) and As(III) adsorption. In the spectrum of pristine adsorbent, the broad band at 3350 cm^{-1} is attributed to the O–H stretching vibration, and the band at 1635 cm^{-1} can be assigned to the bending vibration of H–O–H (water molecule), indicating the presence of physisorbed water on the adsorbent [4]. The bands at 2922 cm^{-1} and 1427 cm^{-1} are attributed to the C–H stretching and bending vibration, respectively [30], which is due to the addition of PVA in the adsorbent. The strong bands at 1115 cm^{-1} and 1060 cm^{-1} can be assigned to the bending vibration of hydroxyl group on metal oxides (M–OH) [2]. Because of the presence of PVA in the adsorbent, the characteristic peak at 1115 cm^{-1} may be attributed to the hydroxyl groups in PVA [30]. The broad band at around 500 cm^{-1} is characteristic of metal–oxygen vibration, which is attributed to the groups of Ti–O and Ce–O in the adsorbent [18,31]. After As(V) and As(III) adsorption, the peak at 3350 cm^{-1} shifted to 3337 cm^{-1} and 3336 cm^{-1}, respectively. The peak at 1060 cm^{-1} disappeared; the peak at 1115 cm^{-1} decreased to 1105 cm^{-1} for As(V) and As(III), and the peak intensity also decreased, indicating that the hydroxyl groups on the adsorbent surface were involved in the arsenic sorption [2,18]. Some researchers have also reported that the peak of hydroxyl groups decreased or disappeared after the sorption arsenic on the Fe–Ce and Fe–Mn adsorbents [2,32]. The peak at 563 cm^{-1} attributed to Ti–O and Ce–O groups decreased to 499 cm^{-1} after As(V) sorption and increased to 595 cm^{-1} after As(III) sorption, suggesting the change of M–O groups after the sorption. It should be pointed out that the As–O band at about 800 cm^{-1} after arsenic sorption was not clearly observed due to the broad overlapping peaks in this region.

To obtain further insight into the arsenic sorption on the Ce–Ti oxide adsorbent, XPS spectra of the adsorbent before and after As(V) and As(III) sorption at pH 6.5 were analyzed. The O 1s, Ti 2p, Ce 3d and As 3d narrow scans are illustrated in Fig. 6. In the Ce–Ti adsorbent sample, the O 1s spectrum was divided into four peaks positioned at 530.1 eV, 531.4 eV, 532.4 eV, and 533.2 eV, which can be assigned to metal oxide (M–O,), hydroxyl bonded to metal (M–OH), hydroxyl in PVA (C–OH), and adsorbed H_2O in the adsorbent (H_2O), respectively [2,33,34]. After arsenic sorption, it can be found that the area ratios of the peaks at 532.4 eV and 533.2 eV changed in a minor way, indicating that the hydroxyl in PVA and adsorbed H_2O were not involved in arsenic sorption, but the area ratio for the peak at 531.4 eV attributed to M–OH decreased from 27.8% to 20.3% and 17.0% after As(V) and As(III) sorption, respec-

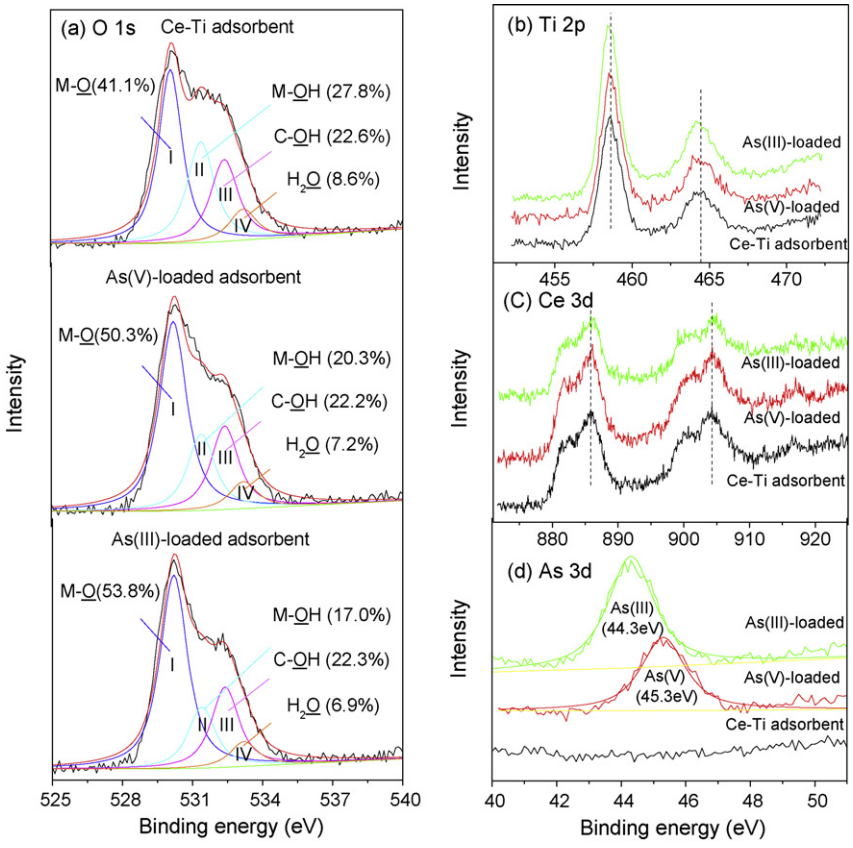

Fig. 6. XPS (a) O1s, (b)Ti 2p, (c) Ce 3d, and (d) As 3d core-level spectra on the Ce–Ti oxide adsorbent surface before and after As(V)/As(III) adsorption at pH 6.5.

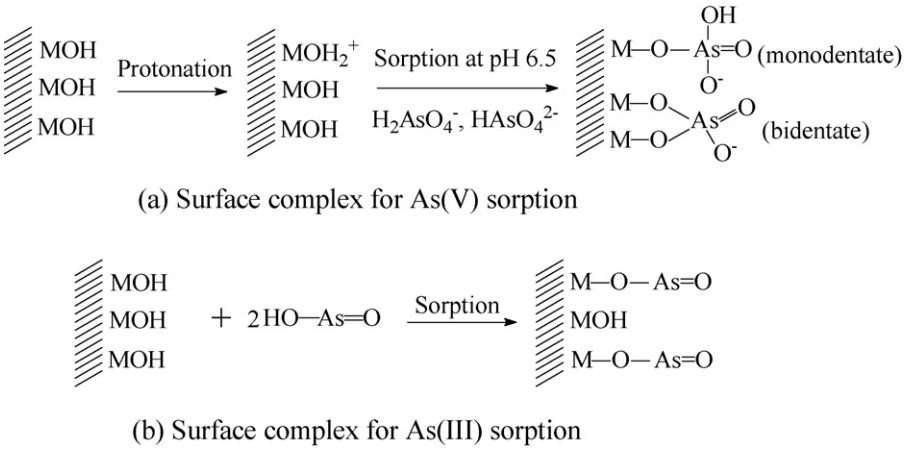

Fig. 7. Schematic diagram for the possible complexes of As(V) and As(III) formed on the Ce–Ti oxide adsorbent (M represents Ce or Ti).

tively. By contrast, the area ratio of the peak at 530.1 eV assigned to M–O increased from 41.1% to 50.3% after As(V) sorption, and reached 53.8% after As(III) sorption. Since As(V) mainly exists as $H_2AsO_4^-$ and $HAsO_4^{2-}$, and As(III) exists as $HAsO_2$ at pH 6.5, one or two As–OH groups are present in one arsenic molecule. Therefore, arsenic adsorption on the adsorbent should increase the area ratio of M–OH if no hydroxyl groups on the metal oxide disappear in the sorption process. The significant decrease of area ratio of the peak at 531.4 eV suggested that the M–OH groups on the adsorbent surface surely participated in arsenic sorption, and the hydroxyl groups in the arsenate and arsenite molecules were also possibly involved in the sorption. The increase of the area ratio for the peak at 530.1 eV may be due to the formation of M–O groups on the adsorbent surface after arsenic sorption, but the As–O groups in the adsorbed arsenic species may also cause this increase since the As–O group has a binding energy at around 530 eV [33]. It is noticeable that the area ratio changes of the two peaks at 531.4 eV and 530.1 eV after As(III) sorption are more obvious than that after As(V) sorption, possibly attributed to the presence of fewer hydroxyl groups in arsenite and more M–OH groups on the adsorbent surface involved in the sorption.

Fig. 6b illustrates the Ti 2p spectra of the adsorbent before and after arsenic adsorption, and the binding energies of 458.6 eV and 464.3 eV for Ti 2p in the spectrum of the Ce–Ti adsorbent can be attributed to Ti $2p_{3/2}$ and Ti $2p_{1/2}$, respectively, indicating the existence of Ti(IV) in TiO_2 [34]. After As(V) sorption, the minor peak for Ti $2p_{1/2}$ shifted to lower binding energy and became unsymmetrical, while the two peaks for Ti $2p_{3/2}$ and Ti $2p_{1/2}$ moved to lower binding energies after As(III) sorption, suggesting that the possibility that the hydroxyl groups bonded to Ti were involved in arsenic sorption and the Ti–O groups at low binding energies formed. The Ce 3d spectra of the adsorbent before and after arsenic adsorption were compared in Fig. 6c. Two pairs of spin-orbital doublets corresponding to the Ce $3d_{3/2}$ and Ce $3d_{5/2}$ contribution were observed, and the peak at 916.8 eV corresponding to Ce(IV) was very weak, indicating that the dominant chemical state of Ce in the Ce–Ti adsorbent was Ce(III) because Ce(IV) in CeO_2 had three pairs of spin-orbital doublets [2]. The Ce 3d spectra of the adsorbent after As(V) and As(III) adsorption showed a small shift at 885.5 eV and 904.5 eV, implying that the groups bonded to Ce also participated in arsenic sorption. The As 3d spectra of the three samples are shown in Fig. 6d, and the remarkable increase of the arsenic signal after sorption verified its successful binding to the adsorbent surface. Only one peak can be assigned to the spectrum of As-loaded adsorbent, and the binding energies at 45.3 eV and 44.3 eV should be ascribed to As(V) and As(III), respectively [35]. This result indicated that As(III) was not oxidized into As(V) during the sorption process. Pena et al. reported that As(III) was converted to As(V) in the presence of sunlight and dissolved oxygen when the naocrystalline TiO_2 was used as an adsorbent [9], but no oxidation reaction occurred in our study as the sorption experiments were conducted under dark conditions.

According to the above zeta potential, FTIR, and XPS analysis, it can be concluded that the hydroxyl groups on the Ce–Ti oxide adsorbent surface are responsible for arsenic sorption, and possible sorption mechanisms are illustrated in Fig. 7. Since the hydroxyl groups on the adsorbent can be protonated in acidic solution, the negative arsenate species ($H_2AsO_4^-$ and $HAsO_4^{2-}$) can be adsorbed on the positive sites on the adsorbent via electrostatic attraction. In consideration of the high sorption capacity of As(V) in acidic solution and significant decrease of sorption capacity at pH above 6.7 in Fig. 2, electrostatic interaction should play an important role in As(V) sorption. At the same time, the M–OH groups on the adsorbent surface are also involved in As(V) sorption via the formation of monodentate and bidentate complexes between As–OH and M–OH and the corresponding M–O groups formed, which is consistent with the decrease of M–OH and increase of M–O in Fig. 6a. In Fig. 2b, the zero points of zeta potential were shifted to pH 4.4 and pH 4.6 after As(V) and As(III) sorption, respectively, indicating the formation of inner-sphere complexes on the adsorbent [36]. Previous studies have shown that activated alumina and iron oxides adsorbed As(V) through the formation of inner-sphere surface complexes of monodentate, bidentate mononuclear, and bidentate binuclear, and that hydroxide groups on the surface played an important role [2,7]. By contrast, neutral As(III) ($HAsO_2$) can only adsorb on the Ce–Ti oxide adsorbent via the formation of monodentate complexes. As some M–OH groups disappeared and corresponding M–O groups formed after As(III) sorption, no As–OH groups were introduced on the adsorption sites. This was verified by the much larger decrease in area ratio for M–OH in O 1s spectra and the more obvious shift in Ce 3d and Ti 2p spectra in Fig. 6.

4. Conclusions

The prepared Ce–Ti hybrid oxide adsorbent was composed of nanoparticles in the size range of 100–200 nm, and its main components included titanium dioxide, cerium oxide and PVA. The powder Ce–Ti oxide adsorbent had high sorption capacity up to 7.5 mg/g for As(V) and 6.8 mg/g for As(III) at the equilibrium arsenic concentration of 10 μg/L, much higher than most adsorbents. The sorption mechanism of As(V) and As(III) on the Ce–Ti adsorbent was complex. Electrostatic interaction occurred in As(V) sorption, and the hydroxyl groups bonded to Ce/ Ti played an important role in the sorption of As(V) and As(III) via the formation of inner-sphere

monodentate and bidentate complexes on the adsorbent. The Ce–Ti hybrid adsorbent has a potential application for arsenic removal in water treatment.

Acknowledgments

We thank the Sanyo Electric Co. Ltd. for financial support, and this research was also supported by Program for New Century Excellent Talents in University. The analytical work was supported by the Laboratory Fund of Tsinghua University. We also appreciate Dr. Heidelore Fiedler from the UNEP Chemicals Branch for comment and suggestion.

References

[1] T.F. Lin, J.K. Wu, Adsorption of arsenite and As(V) within activated alumina grains: equilibrium and kinetics, Water Res. 35 (2001) 2049–2057.
[2] Y. Zhang, M. Yang, X.M. Dou, H. He, D.S. Wang, As(V) adsorption on an Fe–Ce bimetal oxide adsorbent: role of surface properties, Environ. Sci. Technol. 39 (2005) 7246–7253.
[3] K. Banerjee, G.L. Amy, M. Prevost, S. Nour, M. Jekel, P.M. Gallagher, C.D. Blumenschein, Kinetic and thermodynamic aspects of adsorption of arsenic onto granular ferric hydroxide (GFH), Water Res. 42 (2008) 3371–3378.
[4] T. Turk, I. Alp, H. Deveci, Adsorption of As(V) from water using Mg–Fe-based hydrotalcite (FeHT), J. Hazard. Mater. 171 (2009) 665–670.
[5] S.M. Maliyekkal, L. Philip, T. Pradeep, As(III) removal from drinking water using manganese oxide-coated-alumina: performance evaluation and mechanistic details of surface binding, Chem. Eng. J. 153 (2009) 101–107.
[6] S.B. Deng, G. Yu, S.H. Xie, Q. Yu, J. Huang, Y. Kuwaki, M. Iseki, Enhanced adsorption of As(V) on the aminated fibers: sorption behavior and uptake mechanism, Langmuir 24 (2008) 10961–10967.
[7] K.H. Goh, T.T. Lim, Z.L. Dong, Enhanced Arsenic Removal by hydrothermally treated nanocrystalline Mg/Al layered double hydroxide with nitrate intercalation, Environ. Sci. Technol. 43 (2009) 2537–2543.
[8] J.A. Munoz, A. Gonzalo, M. Valiente, Arsenic adsorption by Fe(III)-loaded open-celled cellulose sponge: thermodynamic and selectivity aspects, Environ. Sci. Technol. 36 (2002) 3405–3411.
[9] M.E. Pena, G.P. Korfiatis, M. Patel, L. Lippincott, X.G. Meng, Adsorption of As(V) and As(III) by nanocrystalline titanium dioxide, Water Res. 39 (2005) 2327–2337.
[10] L. Cumbal, A.K. Sengupta, Arsenic removal using polymer-supported hydrated iron(III) oxide nanoparticles: role of Donnan membrane effect, Environ. Sci. Technol. 39 (2005) 6508–6515.
[11] B. An, T.R. Steinwinder, D.Y. Zhao, Selective removal of arsenate from drinking water using a polymeric ligand exchanger, Water Res. 39 (2005) 4993–5004.
[12] G.S. Zhang, J.H. Qu, H.J. Liu, R.P. Liu, R.C. Wu, Preparation and evaluation of a novel Fe–Mn binary oxide adsorbent for effective arsenite removal, Water Res. 41 (2007) 1921–1928.
[13] B.K. Biswas, K. Inoue, K.N. Ghimire, H. Kawakita, K. Ohto, H. Harada, Effective removal of arsenic with lanthanum(III) and cerium(III)-loaded orange waste gels, Sep. Sci. Technol. 43 (2008) 2144–2165.
[14] M. Pena, X.G. Meng, G.P. Korfiatis, C.Y. Jing, Adsorption mechanism of arsenic on nanocrystalline titanium dioxide, Environ. Sci. Technol. 40 (2006) 1257–1262.
[15] S.B. Deng, Z.J. Li, J. Huang, G. Yu, Preparation, characterization and application of a nanostructured Ce–Ti adsorbent for enhanced removal of arsenate from water, J. Hazard. Mater. (2010) 106, doi:10.1016/j.jhazmat.2010.03.
[16] X.M. Wu, Y. Zhang, X.M. Dou, M. Yang, Fluoride removal performance of a novel Fe–Al–Ce trimetal oxide adsorbent, Chemosphere 69 (2007) 1758–1764.
[17] J. Lim, Y. Chang, J. Yang, S. Lee, Adsorption of arsenic on the reused sanding wastes calcined at different temperatures, Colloid Surf. A 345 (2009) 65–70.
[18] Y. Zhang, M. Yang, X. Huang, Arsenic(V) removal with a Ce(IV)-doped iron oxide adsorbent, Chemosphere 51 (2003) 945–952.
[19] P.K. Dutta, A.K. Ray, V.K. Sharma, F.J. Millero, Adsorption of arsenate and arsenite on titanium dioxide suspensions, J. Colloid Interf. Sci. 278 (2004) 270–275.
[20] D. Mohan, C.U. Pittman, Arsenic removal from water/wastewater using adsorbents—a critical review, J. Hazard. Mater. 142 (2007) 1–53.
[21] M. Badruzzaman, P. Westerhoff, D.R.U. Knappe, Intraparticle diffusion and adsorption of arsenate onto granular ferric hydroxide (GFH), Water Res. 38 (2004) 4002–4012.
[22] K.D. Hristovski, P.K. Westerhoff, J.C. Crittenden, L.W. Olsow, Arsenate removal by nanostructured ZrO_2 spheres, Environ. Sci. Technol. 42 (2008) 3786–3790.
[23] T. Balaji, T. Yokoyama, H. Matsunaga, Adsorption and removal of As(V) and As(III) using Zr-loaded lysine diacetic acid chelating resin, Chemosphere 59 (2005) 1169–1174.
[24] H.S. Altundogan, S. Altundogan, F. Tumen, M. Bildik, Arsenic removal from aqueous solution by adsorption on red mud, Waste Manage. 20 (2000) 761–767.
[25] T.S. Singh, K.K. Pant, Equilibrium, kinetics and thermodynamic studies for adsorption of As(III) on activated alumina, Sep. Purif. Technol. 36 (2004) 139–147.
[26] V. Lenoble, C. Laclautre, B. Serpaud, V. Deluchat, J.C. Bollinger, As(V) retention and As(III) simultaneous oxidation and removal on a MnO_2-loaded polystyrene resin, Sci. Total Environ. 326 (2004) 197–207.
[27] S. Ayoob, A.K. Gupta, P.B. Bhakat, Performance evaluation of modified calcined bauxite in the sorptive removal of arsenic(III) from aqueous environment, Colloid. Surf. A 293 (2007) 247–254.
[28] S.B. Deng, Y.P. Ting, Polyethylenimine-modified fungal biomass as a high-capacity biosorbent for Cr(VI) anions: Sorption capacity and uptake mechisms, Environ. Sci. Technol. 39 (2005) 8490–8496.
[29] C.A. Martinson, K.J. Reddy, Adsorption of arsenic(III) and arsenic(V) by cupric oxide nanoparticles, J. Colloid Interf. Sci. 336 (2009) 406–411.
[30] M. Abdelaziz, E.M. Abdelrazek, Effect of dopant mixture on structural, optical and electron spin resonance properties of polyvinyl alcohol, Physica B 390 (2007) 1–9.
[31] J.P Nikkanen, T. Kanerva, T. Mantyla, The effect of acidity in low-temperature synthesis of titanium dioxide, J. Cryst. Growth 304 (2007) 179–183.
[32] G.S. Zhang, J.H. Qu, H.J. Liu, R.P. Liu, G.T. Li, Removal mechanism of As(III) by a novel Fe–Mn binary oxide adsorbent: oxidation and sorption, Environ. Sci. Technol. 41 (2007) 4613–4619.
[33] E.A. Deliyanni, L. Nalbandian, K.A. Matis, Adsorptive removal of arsenites by a nanocrystalline hybrid surfactant–akaganeite sorbent, J. Colloid Interf. Sci. 302 (2006) 458–466.
[34] S.F. Lim, Y.M. Zheng, J.P. Chen, Organic arsenic adsorption onto a magnetic sorbent, Langmuir 25 (2009) 4973–4978.
[35] E.J. Kim, B. Batchelor, Macroscopic and X-ray photoelectron spectroscopic investigation of interactions of arsenic with synthesized pyrite, Environ. Sci. Technol. 43 (2009) 2899–2904.
[36] S. Goldberg, C.T. Johnston, Mechanisms of arsenic adsorption on amorphous oxides evaluated using macroscopic measurements, vibrational spectroscopy, and surface complexation modeling, J. Colloid Interf. Sci. 234 (2001) 204–216.